

## TWO-DIMENSIONAL ENDFIRE ARRAY WITH INCREASED GAIN AND SIDE LOBE REDUCTION

H. W. Ehrenspeck  
W. J. Kearns

Antenna Laboratory  
Electronics Research Directorate  
Air Force Cambridge Research Center (ARDC)  
Laurence G. Hanscom Field, Bedford, Mass.

### Summary

Endfire arrays such as Yagi antennas can be analyzed in terms of the phase and amplitude distribution in a "virtual aperture" plane transverse to the axis of the array. A method for controlling the amplitude and phase across the virtual aperture is given. It is shown, in particular, that the virtual aperture area can be increased through the use of parasitic side arrays, and that at the same time control of the illumination function can be retained. Thus, it is possible to increase gain and reduce side lobes simultaneously without supergaining.

Measured patterns are shown for three different array types. Type I is a Yagi antenna 6 wavelengths long, tuned for maximum gain by using a modified Hansen-Woodyard condition reported elsewhere.<sup>7</sup> Types II and III are two-dimensional endfire arrays, also 6 wavelengths long. Type II was tuned for very low side lobe level (30 db), and Type III for maximum gain obtainable with a more moderate side lobe level (17 db). The gain of Type II was 30% above that of Type I, while the gain of Type III was 60% above Type I.

The method presented demonstrates that controlled excitation of a two-dimensional parasitic array with a single feed (rather than a line source) is feasible.

### 1. Introduction

The performance of an endfire array such as a Yagi antenna<sup>1-8</sup> depends on a number of parameters: on the choice of the reflector, on the height (length), diameter, and spacing of the parasitic elements, and on the length of the array. It was shown in an earlier report<sup>7</sup> that the connection between the parameters height, diameter, and spacing can be described by introducing the notion of a surface wave traveling along the array with a certain phase velocity which in itself is a function of these parameters. The gain of an endfire array of this type then depends only on the phase velocity, which has to be optimized for any given array length, and which is always slower than the velocity of light.

An endfire array of this type acts like a traveling wave antenna. The energy is concentrated in a channel along the line of parasitic

elements and guided along the array from the feed to the end. Radiation takes place because of the finiteness of the structure. Figure 1, an amplitude and phase plot of the near field of a Yagi array shows this effect very clearly. The Yagi antenna used in the measurement has a length of  $6\lambda$  and is adjusted for maximum gain in the endfire direction according to the design method given in<sup>7</sup>. For reasons which are mentioned in Section 6 all measurements were taken above a large ground plane. The points show the location of the parasitic elements called directors, which are brass rods sticking out perpendicularly from a large metal ground plane. The spacing between the elements is  $0.200\lambda$ ; their diameter is  $0.048\lambda$ . The lines A, B, C, and D, parallel to the symmetry axis of the array, are lines of constant amplitude, plotted in steps of 5 db. The energy level of line D is then 20 db below the reference level located near the feed. The lines perpendicular to the direction of propagation are constant phase contours, plotted at  $360^\circ$  intervals.

The plot shows that the energy is very strongly concentrated along the line of directors. The field decreases exponentially in the direction perpendicular to the propagation and has dropped to 20 db at a distance of only 1 wavelength from the line of directors. The decrease is more pronounced the more the phase velocity differs from the velocity of light. It can also be clearly seen that, with the exception of a negligible amount near the feed, very little energy is radiated along the array. Only at the array end does the energy begin to spread out.

### 2. The "Virtual Wave Channel" of a Long Yagi Antenna

If we assume that power levels more than 20 db below maximum do not make substantial contributions to the far field pattern of the array, an assumption, which is often made in the literature, we can say that apart from the direct feed radiation all of the energy travels along the array in a virtual wave channel which in our case, has an overall width of about 2 wavelengths. In Fig. 1 we see the dimensions of this wave channel in the horizontal plane. It will be shown later

that the wave channel has about the same dimensions in the vertical plane. The wave channel is therefore like a tube with circular cross section. The energy transported through the channel is radiated at the open end of the tube just as from the open end of a waveguide or the mouth of a horn. It should be noted, however, that the field propagating in this wave channel is not purely in the form of a single mode (the surface wave), but is accompanied by a non-negligible perturbation arising from the region of the feed.

### 3. The "Virtual Aperture" of an Endfire Array

Let us now consider the end of the array as a radiating aperture. Because this aperture has no physical limits, one can only speak of it as a "virtual aperture." It seems reasonable to define the extent of the virtual aperture in the same manner as was done for the width of the wave channel, that is, we take into consideration only that part of the energy flow which is not more than 20 db below the maximum.

In this manner we can express the width of the virtual aperture per wavelength of an endfire array just as we usually do in the case of a broadside array.

### 4. Amplitude and Phase Distribution in the Virtual Aperture of an Endfire Array

It follows from these results that instead of regarding the gain and the pattern of an endfire array as a function of the array length and of the phase velocity along it, we can regard it as a function of the amplitude and phase distribution in the virtual aperture.

We conclude therefore that we can change both gain and pattern, provided we find a way to change the width of the virtual aperture and its amplitude and phase distribution. By thus passing from a one to a two-dimensional array, we can increase the gain by increasing the virtual aperture, or reduce side lobes by changing the amplitude and phase distribution in the proper manner. We can, furthermore, get increased gain and reduced side lobes simultaneously by changing both the width and the aperture distribution.

### 5. A Method for Increasing the Virtual Aperture and Changing the Aperture Distribution

It was found that the width of, and distribution in, the virtual aperture can be changed in the desired manner by symmetrically placing one or more shorter rows of parasitic elements on either side of the center array. These act as smaller wave channels fed by coupling from the main array. We now have a two-dimensional parasitic endfire array, excited only by the single feed of the main array. Figure 2 shows a sketch of such an array indicating the directions in the virtual aperture in which measurements were taken. It also shows the limitations of the virtual aperture in both the transverse and vertical directions.

The side rows have to be adjusted so that the phase front in the virtual aperture is as uniform as possible and the amplitude distribution is given

the form needed for the specified pattern. Fortunately, both parts of the adjustment can be performed within limitations independently of each other: the phase is controlled by adjusting the phase velocity (which depends on the spacing, height, and diameter of the parasitic elements), and the amplitude by the length of the side rows.

### 6. Experimental Arrangement

Because it was necessary to have an arrangement by which the different parameters of the yagi and the two-dimensional array could be easily changed, it was decided to perform the experiments above a ground plane. This offers many advantages one of which is the feeder arrangement which can be excited from beneath and is coaxially connected. The mechanical support of the elements was furnished by the ground plane, in which a series of holes were drilled. The individual radiators were press-fit brass rods inserted in the holes, their height was experimentally adjusted. The spacing between elements could easily be changed in multiples of the smallest separation which was  $.100\lambda$ .

As the pattern and gain would have to be measured in the far field the ground plane was extended as far out as feasible. To keep the dimensions reasonable it was decided to use X-band (3.3 cm), and because of the directive nature of the antennas, a width of six feet and a length of twelve feet (110 wavelengths) was chosen.

In order that far field patterns could be taken, the set of holes that held the elements were drilled in a circular plate recessed in the previous mentioned ground plane. This in turn was connected to an antenna mount in such a fashion that the array under observation could be rotated while a receiving antenna which was fixed to the far end of the ground plane detected the signal and relayed it to an antenna pattern recorder.

The amplitude and phase measurements taken in the aperture plane were conducted by the use of a small dipole probe mounted in a perpendicular position and moved in the H-plane at a constant distance of about  $\lambda/4$  above the ground plane.

The plots of amplitude and phase shown in this report were obtained with the automatic plotter designed and built at the Air Force Cambridge Research Center.<sup>9</sup>

All experiments were conducted in a microwave dark room and the ground plane was further surrounded by absorbing material to reduce reflections to a minimum. The results of these experiments were taken and often repeated on different days with a relative error of  $\pm 0.1$  db. All mechanical tolerances pertinent to the measurements were held to  $\pm 0.001$  of an inch.

### 7. Measurement of Amplitude and Phase Distribution in the Virtual Aperture of Three Types of Endfire Arrays

Measurements of amplitude and phase distribution were performed on three different types of endfire arrays:

Type I, a Yagi-type endfire array  $6\lambda$  long,  
adjusted for maximum gain.<sup>7</sup>

Type II, a two-dimensional endfire array with two parasitic side rows.

Type III, a two-dimensional endfire array with six parasitic side rows.

The most important physical dimensions of these three array types are shown in Fig. 3.

### 7.1 Yagi-Type Endfire Array (Type I)

Figure 4a and b show the measured amplitude and phase distribution in the virtual aperture of array Type I. Because of the symmetry of the array only half of the distribution curve is shown. Looking at Fig. 4a we notice that the amplitude first decreases exponentially from its maximum value on the symmetry axis of the array. Further out from the axis, at a distance of about  $1\lambda$ , the decrease becomes slower. According to the aperture definition given in Sec. 3, the width of the virtual aperture is  $2.78\lambda$ .

The phase distribution curve, shown in Fig. 4b indicates phase changes between  $+30^\circ$  and  $-30^\circ$  within the virtual aperture. Greater phase changes exist outside the virtual aperture, but because the amplitude level is more than 20 db below the maximum, these phase changes cannot have an important influence on the pattern (except on the far-out side lobes).

### 7.2 Two-Dimensional Endfire Arrays (Types II and III)

If we add side arrays to this endfire antenna in the manner described in Section 5, the amplitude and phase distribution in the virtual aperture as well as the aperture width are changed; therefore, gain and side lobe level of the array are changed simultaneously. It follows that the measurement of the gain in the endfire direction is not a sufficient criterion for the optimum adjustment of the array. It was decided first to adjust the side rows so that the side lobes of the two-dimensional array were decreased to the lowest measurable value. The aperture distribution required for a radiation pattern without side lobes is a uniform phase front and a Gaussian amplitude distribution.<sup>10</sup>

If, therefore, we measure radiation patterns with extremely low side lobes, one can draw the conclusion that the aperture distribution of this array should be very nearly Gaussian. We will show later that this is so.

Looking at Fig. 4b, the best location for the side arrays would seem to be at a point within the virtual aperture where the phase had deviated most from the phase reference point on the array axis. This point is at a distance of  $2/3\lambda$  from the array axis. The side rows then have to be adjusted so that the wave guided along them travels faster than the wave in the main array by such an amount so as to produce as nearly constant a phase front in the aperture as possible. Furthermore, the lengths of the side rows have to be adjusted so that the amplitude distribution in the virtual aperture plane of the new two-dimensional endfire array is as nearly Gaussian as possible. Because of the very complicated influence of the side rows on the main array,<sup>11</sup> the correct length of the side rows can be found only by experiments.

As mentioned before, we adjusted for the lowest possible side lobes and checked only afterwards to see how closely the measured distribution curve compared to the Gaussian. Figure 5 shows the amplitude and phase distribution in the virtual aperture of the two-dimensional endfire array with two side rows, each at a distance of  $2/3\lambda$  from the symmetry line (Array Type II). We notice that the virtual aperture of the array has increased from  $2.78\lambda$  to  $3.82\lambda$ , an increase of 37%. The phase distribution curve is now more uniform than it was with the original Yagi. The phase in this case has no maximum and minimum and changes smoothly within the virtual aperture plane. The measured increase in gain was found to be about 30%. The physical dimensions of the array are given in Fig. 3.

In addition to this array with two side rows, another one with six side rows was constructed (Array Type III). The amplitude and phase distributions are shown in Fig. 6. We notice that the virtual aperture has increased to  $4.62\lambda$ , an increase of 66% above the Yagi-type endfire array, and the measured gain increase was about 60%.

### 8. Comparison of Measured Transverse Amplitude Distribution Curves for the Virtual Aperture of Array Types I, II, and III with the Gaussian Distribution

Figure 7 shows the amplitude distribution curves measured in the transverse direction of the virtual aperture of the array Types I, II, and III. These curves are given on a linear scale and normalized for equal virtual aperture width according to the definition in Section 3. The thin line indicates the Gaussian distribution. It may be seen that the distribution for array Type II approaches the Gaussian better than the distribution for array Type I. An obvious conclusion is that array Type I must have much higher side lobes than array Type II. According to our measurements the side lobe level was only 10 db below maximum for array Type I, but about 30 db below maximum for Type II.

The distribution for array Type III is again more remote from the Gaussian, signifying higher side lobes once more. In the measurements the side lobe level of array Type III was 17 db below maximum (the gain was increased at the same time by 2.1 db). These results were taken from measured far-field patterns shown later in Fig. 13 to Fig. 15.

### 9. Vertical Amplitude Distribution in the Virtual Aperture of Array Types I, II, and III

Until now the discussion has been concerned with the virtual aperture distribution in the transverse direction. For a complete aperture description we also need to know the energy distribution in the vertical direction. Figure 8 shows the amplitude distribution in the vertical direction of the virtual aperture for array Types I, II, and III. For comparison, the corresponding ampli-

tude distributions in the transverse direction are found on the right. We notice that in the vertical direction the aperture distribution is essentially the same for all three array types. The three curves indicate only small differences that are found near the rim of the virtual aperture, where the energy has dropped to 20 db. We conclude that the side rows, which were used for producing a certain aperture distribution in the transverse direction, have no essential influence on the distribution in the vertical direction. It follows that no new side lobes will arise in the E-plane far-field pattern when we reduce or suppress the side lobes in the H-plane with parasitic side rows. If we wish to increase the width of the virtual aperture in the vertical direction, we will have to place side rows above the main array (and below, if there is no ground plane). By thus passing from a two to a three-dimensional array, the gain could be increased even further.

#### 10. Influence of Side Rows on the Near-Field of Two-Dimensional Endfire Arrays

It was shown qualitatively in Fig. 1 that the line of parasitic elements in an endfire array acts like a wave channel in which the energy is guided from the feed to the end of the array, and is radiated there. For this reason the vertical aperture plane is located such that the last director is found in its center. In an endfire array, longer than about  $3\lambda$ , consisting of parasitic elements of equal spacing, diameter, and height, the dimensions of the wave channel remain constant along the length of the array, except in the region very near the feeder-reflector combination. We arrive at this statement by noting that the lines of constant energy run parallel to the line of directors except near the feed region.

When we pass to the two-dimensional array with side rows, the dimensions and the distribution in the wave channel change along the length of the array. A very complicated form of coupled power flow takes place, which is shown in Fig. 10 and Fig. 11. For comparison we show Fig. 9, the amplitude and phase plot of a Yagi-type endfire array (Type I), which has the same length as the arrays in Fig. 10 and 11.

As in Fig. 1, the horizontal lines are lines of constant amplitude level plotted in 5 db steps. The lines perpendicular to the direction of propagation are phase lines, each spaced  $360^\circ$  from the next. In order to normalize the plots, and thus be able to compare them in amplitude and phase, the plotter was always adjusted so that a small circle with the maximum amplitude was plotted when the test probe moved across the feed, and a phase line was plotted just as the probe passed the last director.

Figures 9 to 11 each show two plots marked A and B. The points lying on the axis of the arrays in plots A, and the corresponding short vertical lines in plots B, indicate the location of the individual elements. Plots A are taken in the transverse plane, spaced  $\lambda/4$  above the ground plane, and plots B are taken in the vertical plane containing the array axis. Taken together they give a two-dimensional picture of the energy distri-

bution along the array and the near-field pattern starting in the virtual aperture plane. We note that the fields in the neighborhood of the parasitic elements are considerably perturbed when two or more side rows are added to the center array. We see also that the cross section of the wave channel varies along the array. And finally we note that the radiated beams of the three array types, starting at the virtual aperture plane, are narrowed by adding side rows. Because we are still in the Fresnel zone, we cannot compare the width of the beams directly.

#### 11. Measurement of the Two-Dimensional Amplitude Distribution in the Virtual Aperture of Array Types I, II, and III

Figure 12 shows a direct measurement of the two-dimensional amplitude contours in the virtual aperture of array Types I, II, and III, marked a, b, and c, respectively. For this measurement the probe was moved in the aperture plane transverse to the center line at increasing heights above the metal ground plane. The lines again indicate points of equal field strength in the aperture, plotted here at intervals of 3 db between contours. The last line is 21 db below the maximum, measured directly above the last director. We can therefore say that this line gives the approximate extent of the virtual aperture in two dimensions. The shape of this 21 db contour is therefore the shape of the virtual aperture itself. We learn from Fig. 12 that the virtual aperture of a one-dimensional endfire array, such as a Yagi, is shaped like a circle with small perturbations on the outside. These perturbations are responsible for the high side lobes in the far field. By inserting the side rows, the shape of the virtual aperture changes to one resembling an ellipse, and the perturbations vanish. The ellipse becomes more and more elongated as further side rows are added.

#### 12. Far-Field Patterns of Array Types I, II, and III

The H-plane far-field patterns of the three arrays are shown in Figs. 13, 14, and 15 for array Types I, II, and III, respectively. The feed-reflector combination used in these measurements consisted of a dipole and a corner reflector. This combination was chosen because of its excellent back lobe reduction. The back lobe level was of the same order of magnitude as the side lobe level of the two-dimensional array.

The most important results obtained from these patterns are displayed in the following table (Table I), which also lists the relative sizes of the virtual apertures.

#### Conclusions

It has been shown in this report that the performance of a long endfire array consisting of linear elements, such as a Yagi antenna, can be understood by the concept of a virtual aperture that is located at the end of the array. It has also been shown that it is possible to accomplish control of this aperture by coupling energy parasitically from the main array into adjacent side

rows disposed along its axis.

Using this method gain and side lobe level of such an endfire array can be changed simultaneously. These accomplishments are obtained by low cost antenna construction and without an appreciable increase in space compared to conventional endfire arrays of the same length. Furthermore, the initial feed system can be used without complicated power distribution networks common to other antennas producing comparable results. Because of its mechanical and electrical simplicity, this antenna type may be used for high as well as low frequencies.

#### REFERENCES

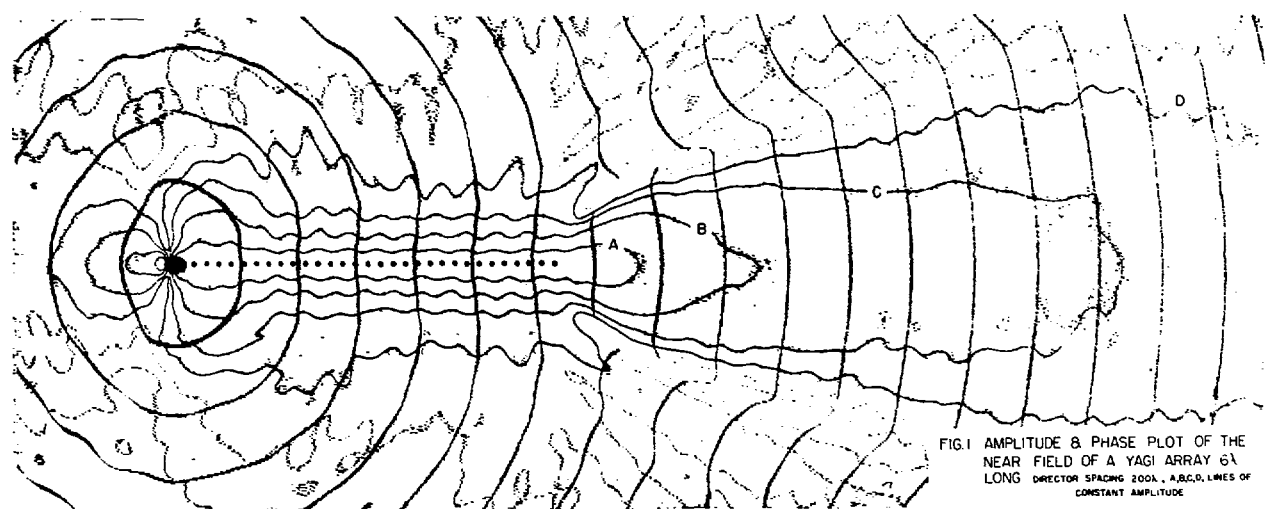
1. H. YAGI, Beam Transmission of Ultra Short Waves. Proc. IRE, 1928, Vol. 16, p. 715.
2. S. UDA and Y. MUSHIAKE, Yagi-Uda Antenna, Sasaki Co., Ltd., 1954 (Japan).
3. R.M. FISHENDEN and E.R. WIBLIN, Design of Yagi Aerials. Proc. I.E.E., Part 3, 1949, Vol. 96, p. 5.
4. D.G. REID, The Gain of an Idealized Yagi Array. Jour. I.E.E., Part 3A, No. 3, Vol. 93, p. 564.
5. D.M. VYSOKOVSKY, Amplitude and Phase Relations of Currents in Coupled Oscillator Antennas. Doklady, A.N. USSR, Vol. 96, No. 5, 1954, p. 971.
6. D.M. VYSOKOVSKY, Resonance in a System of Coupled Oscillators and a Tuned Antenna. Doklady, A.N. USSR, Vol. 97, No. 4, 1954, p. 659.
7. H.W. EHRENSPECK and H. POEHLER, A New Method for Obtaining Maximum Gain From Yagi Antennas. Presented at Wescon 1956, Los Angeles, Cal. by personnel of Antenna Laboratory, ERD, AFCRC, Bedford, Massachusetts.
8. W.W. HANSEN and J.R. WOODYARD, A New Principle in Directional Antenna Design. Proc. IRE, 1938, Vol. 26, p. 333.
9. R.M. BARRETT and M.H. BARNES, Automatic Antenna Wavefront Plotter. Electronics, Vol. 25, Jan. 1952.
10. J.D. KRAUS, Antennas. McGraw-Hill Book Co., Inc., 1950, pp. 93-97.
11. J.H. CRYSDALE and D.J. OLIVE, Some Measurements on the Effects of Interaction between Yagi Antennas. Project Report No. 12-0-1, Defense Research Telecommunications Establishment, Ottawa, Canada.

#### ACKNOWLEDGMENTS

The authors are indebted to Mr. F.J. Zucker, Dr. W. Gerbes, Mr. C.J. Drane, Jr., and Lt. G.B. Parrent for many stimulating discussions. This work was done under the general direction of Mr. F.J. Zucker, Chief of the Airborne Antenna Section, and Mr. Ralph E. Hiatt, Chief of the Antenna Laboratory.

Array Type	Half Power Beam Width	1. Side Lobe db	Back Lobe db	Gain above Dipole db	Relative Size of Virtual Aperture
Yagi Array 6 $\lambda$ Long Type I	20.5°	10	28	14.0	1.00
Two Dimensional End Fire Array 6 $\lambda$ Long with 2 side rows TYPE II	18.5°	30	31	15.1	1.37
Two Dimensional End Fire Array 6 $\lambda$ Long with 6 side rows TYPE III	15.5°	17	26	16.1	1.66

TABLE I. COMPARISON OF ARRAY TYPES



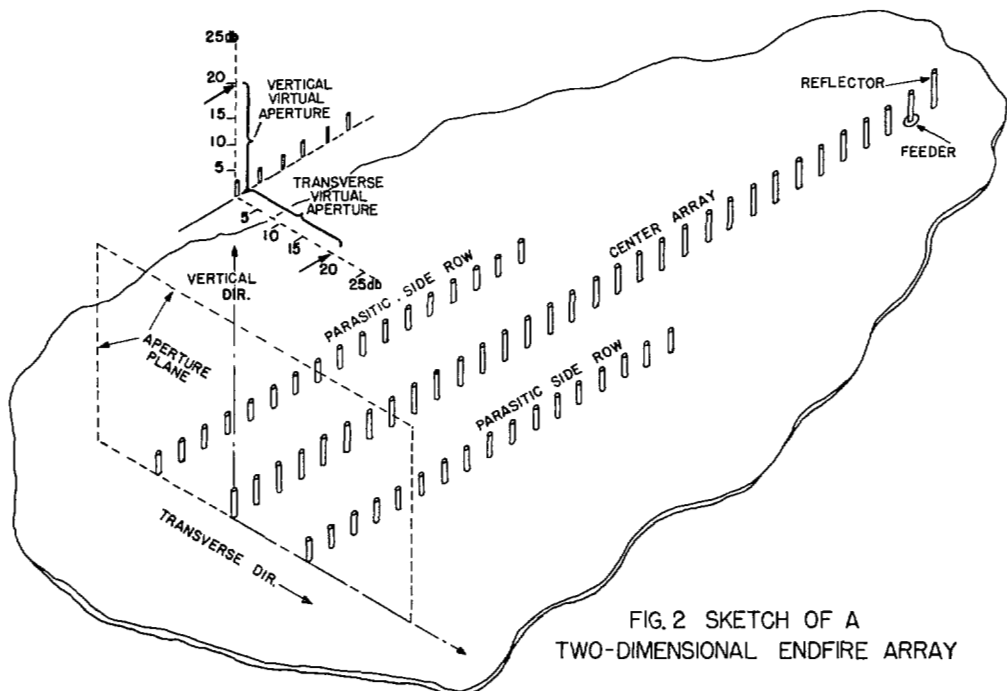


FIG. 2 SKETCH OF A  
TWO-DIMENSIONAL ENDFIRE ARRAY

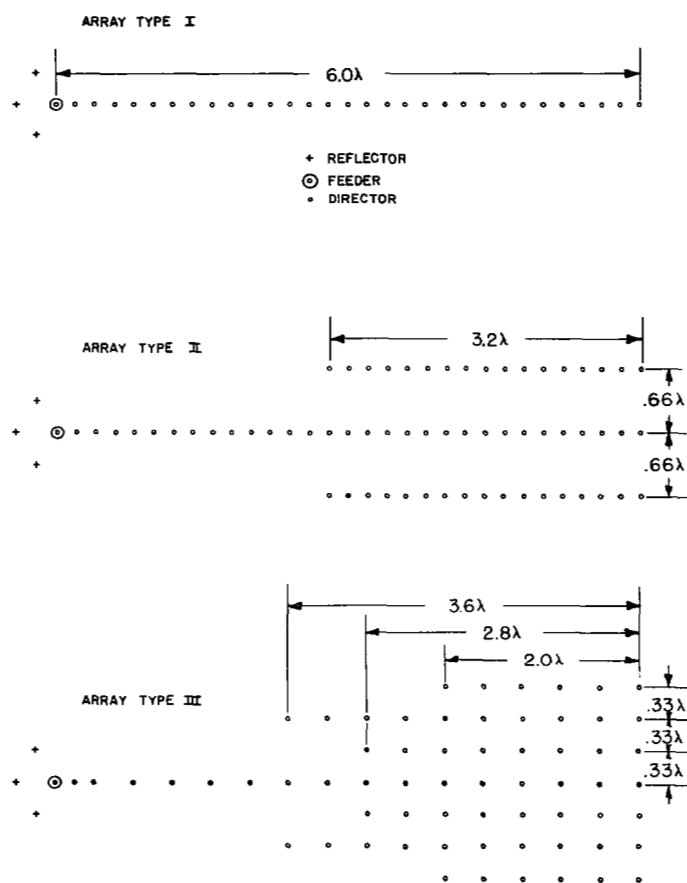


FIG. 3. PHYSICAL DIMENSIONS OF THE ARRAY TYPES  
I, II, AND III

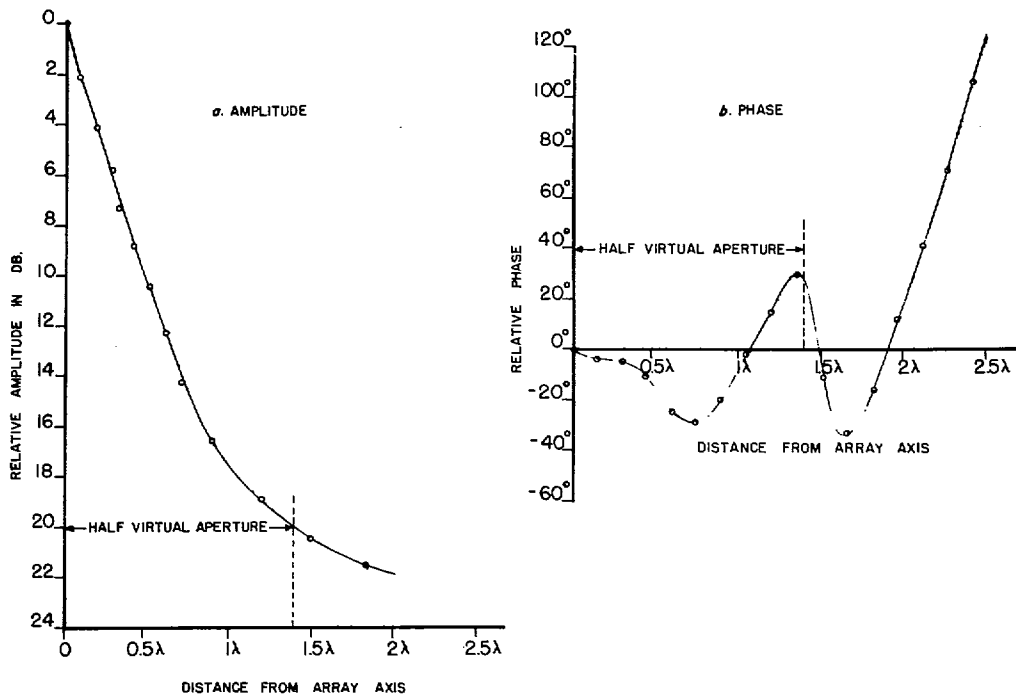


FIG. 4 AMPLITUDE & PHASE DISTRIBUTION IN THE TRANSVERSE DIRECTION OF THE VIRTUAL APERTURE OF A YAGI ANTENNA (TYPE I)  
(MEASURED ALONG GROUND PLANE)

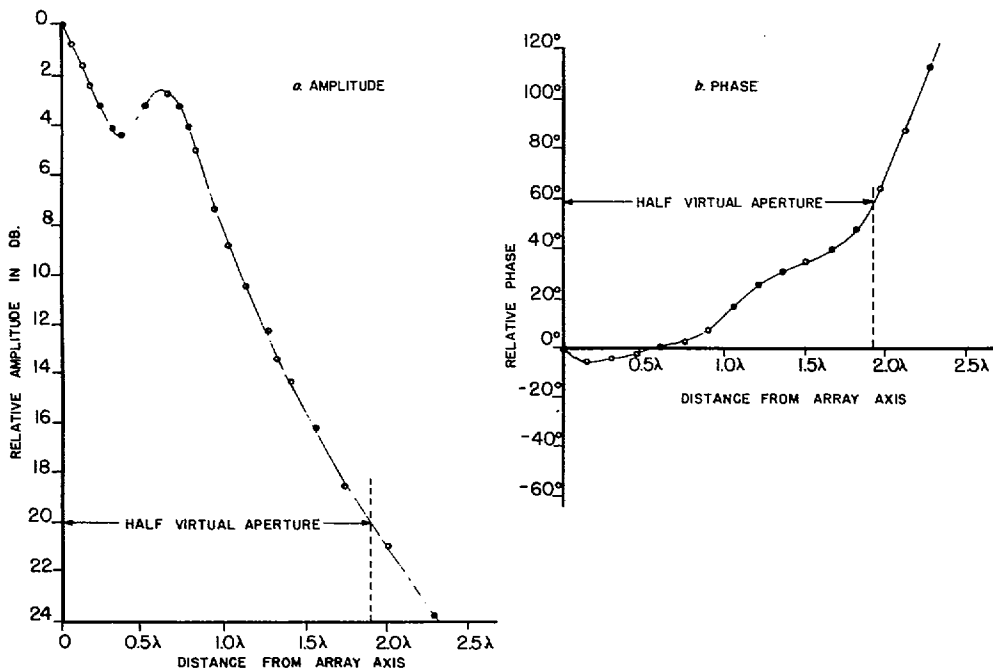


FIG. 5 AMPLITUDE & PHASE DISTRIBUTION IN THE TRANSVERSE DIRECTION OF THE VIRTUAL APERTURE OF A TWO DIMENSIONAL ENDFIRE ARRAY, TYPE II (MEASURED ALONG GROUND PLANE)

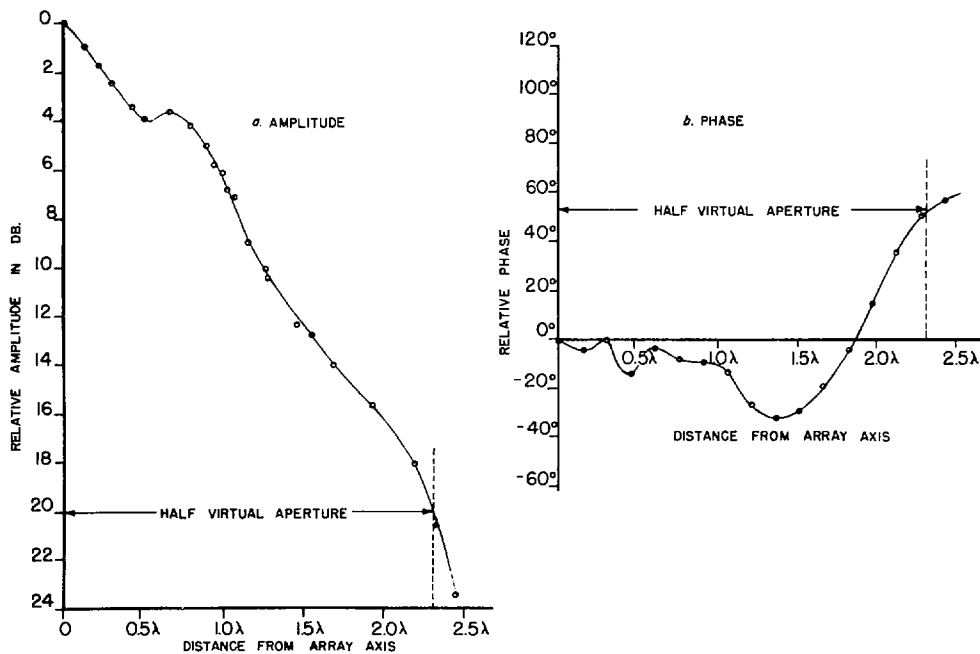


FIG.6 AMPLITUDE & PHASE DISTRIBUTION IN THE TRANSVERSE DIRECTION OF THE VIRTUAL APERTURE OF A TWO DIMENSIONAL ENDFIRE ARRAY, TYPE III  
(MEASURED ALONG GROUND PLANE)

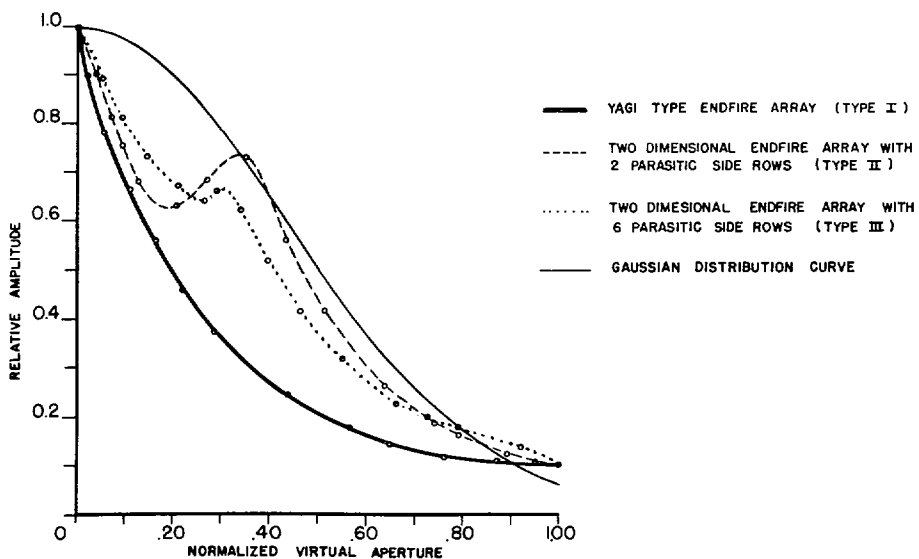


FIG.7 AMPLITUDE DISTRIBUTION IN THE TRANSVERSE DIRECTION OF THE VIRTUAL APERTURE OF ARRAY TYPES I, II, & III (MEASURED ALONG GROUND PLANE, AND NORMALIZED FOR EQUAL APERTURE WIDTHS)

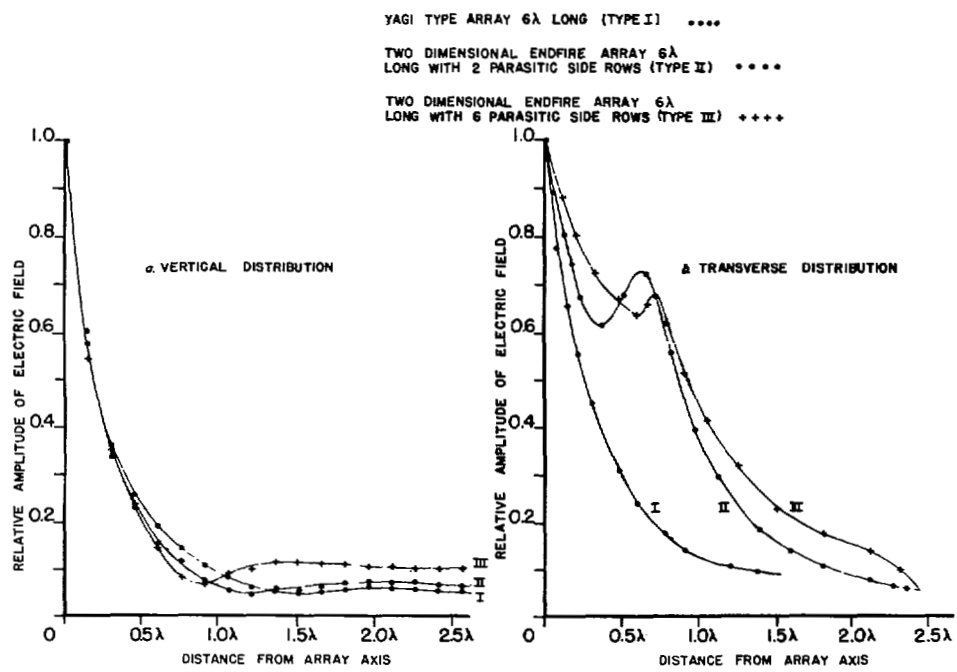


FIG. 8 VERTICAL & TRANSVERSE AMPLITUDE DISTRIBUTION IN THE VIRTUAL APERTURE OF ARRAY TYPES I, II, & III

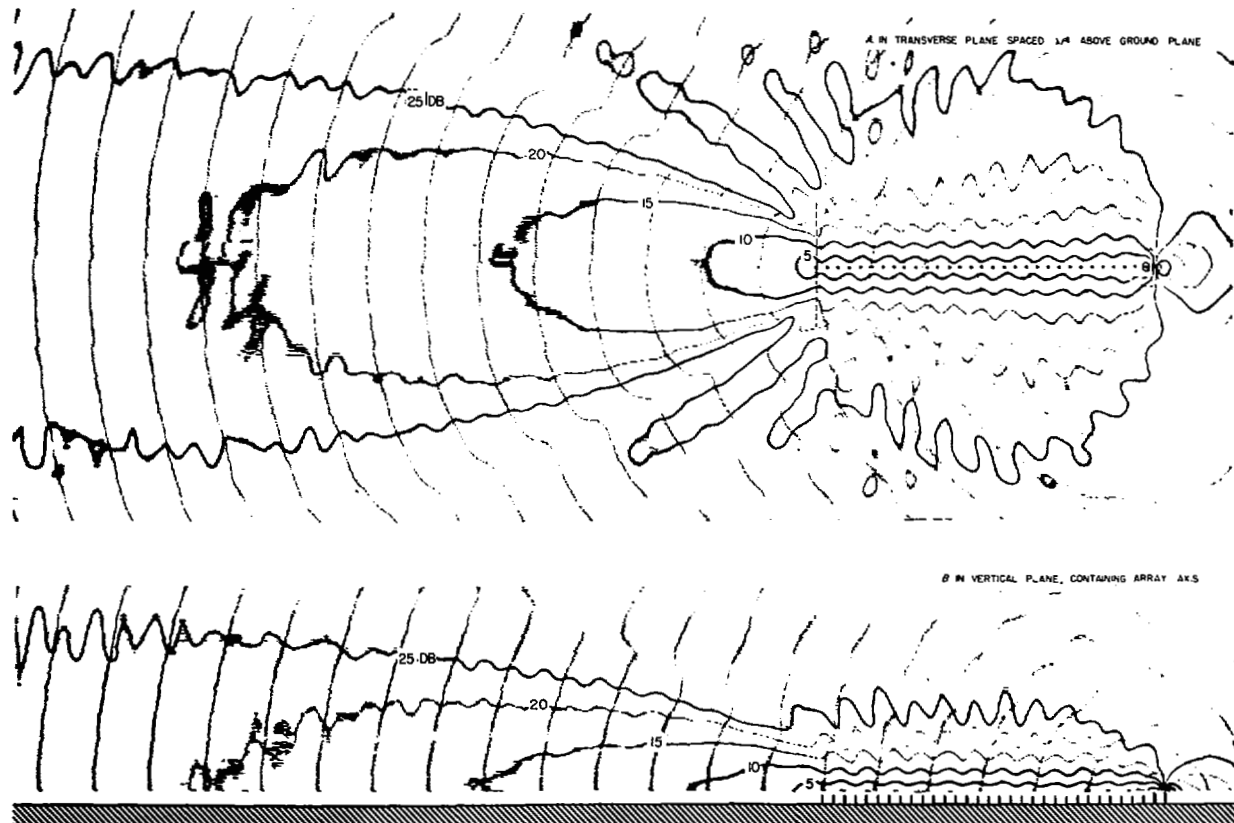


FIG. 9 AMPLITUDE & PHASE PLOTS OF THE NEAR FIELD OF A YAGI ARRAY (TYPE I)

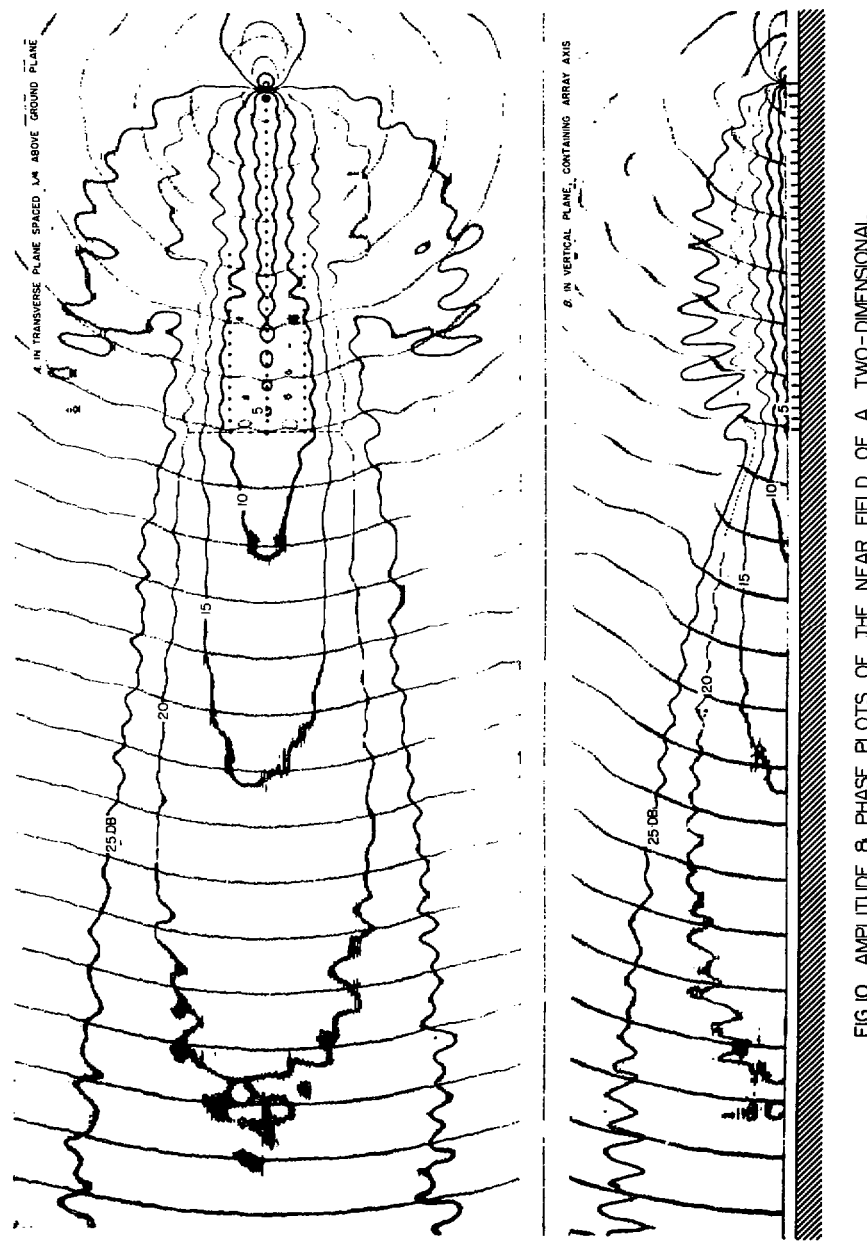


FIG. 10 AMPLITUDE & PHASE PLOTS OF THE NEAR FIELD OF A TWO-DIMENSIONAL ENDFIRE ARRAY (TYPE II)

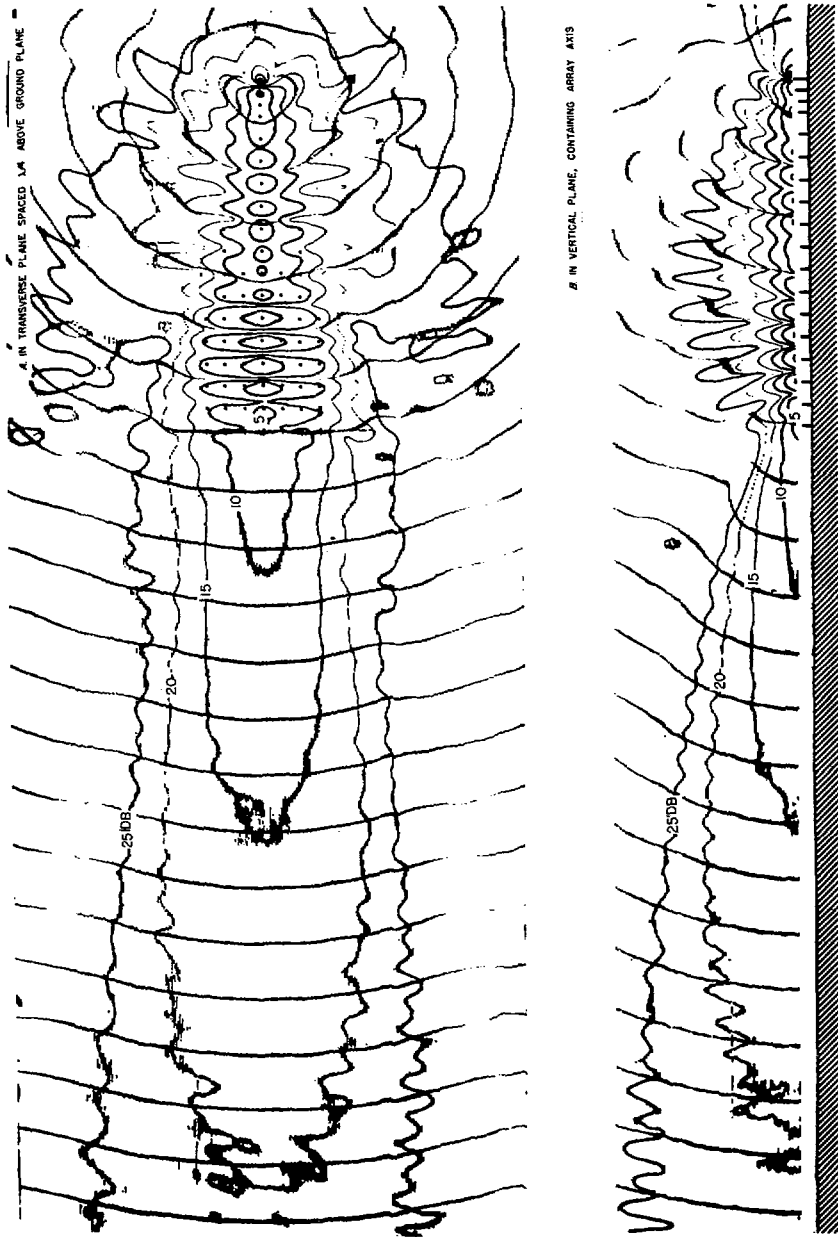


FIG. II AMPLITUDE & PHASE PLOTS OF THE NEAR FIELD OF A TWO-DIMENSIONAL ENDFIRE ARRAY (TYPE III)

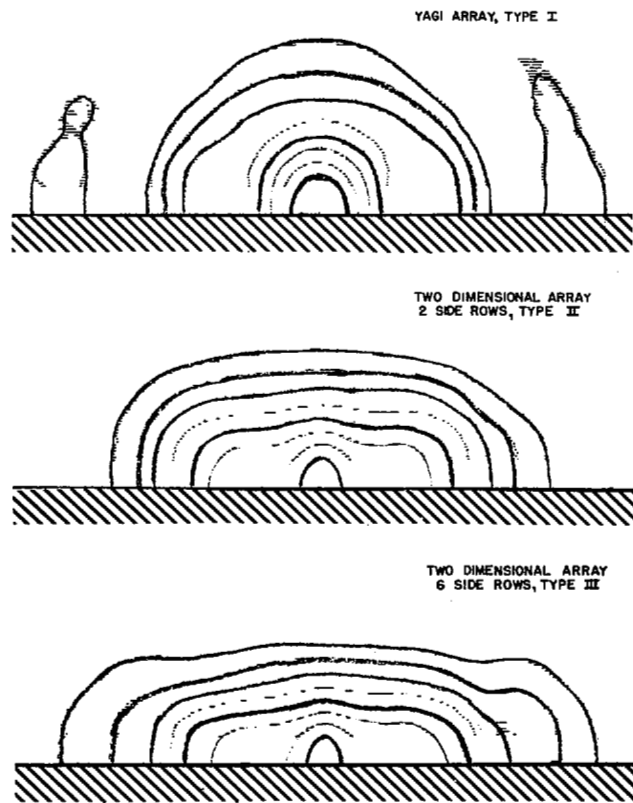


FIG.12 AMPLITUDE CONTOURS IN THE VIRTUAL APERTURE  
OF ARRAY TYPES I, II, & III

